Materials and Structures, 1992, **25**, 84–94

Improved prediction model for time-dependent deformations of concrete: Part 4 – Temperature effects

ZDENĚK P. BAŽANT, AND JOONG-KOO KIM

Center for Advanced Cement-Based Materials, Northwestern University, Evanston, Illinois 60208, USA

This Part presents a refinement of the BP model for the effects of temperature on the basic creep and drying creep of concrete. The temperature effect on basic creep is introduced through two different activation energies, one for the effect of temperature increase on the rate of hydration, which causes a decrease of creep, and one for the effect of temperature increase on the rate of creep, which causes an increase of creep. The dichotomy of these two opposing temperature influences is an essential feature, required for good agreement with test data. The greatest error in basic creep is again caused by the prediction of the material parameters from concrete composition and strength. This error can be largely eliminated by conducting limited short-time basic creep tests at different temperatures. Comparisons with 13 different data sets from the literature show a satisfactory agreement, better than that achieved with previous models, while at the same time the scope of the present model is broader. The effect of temperature on the creep of drying specimens is rather different because heating causes a moisture loss from unsealed specimens. The paper presents prediction formulae which modify those for drying creep at room temperature on the basis of the activation energy concept and take into account the effect of heating on the moisture loss. Comparisons with the limited test data that exist show satisfactory agreement. No additional material parameters depending on concrete composition and strength are introduced for drying creep.

1. INTRODUCTION

Temperature exerts a significant influence on concrete creep. This is particularly important for structures such as concrete reactor vessels or radioactive waste containment, which operate at elevated temperatures. Heating of concrete accelerates creep but it also accelerates hydration which tends to reduce creep. These opposite effects complicate the effect of temperature. Further effects determine that the creep of sealed and unsealed specimens depends on temperature in a different manner. Heating accelerates moisture loss from unsealed specimens, which tends to magnify creep. On the other hand, when an unsealed specimen approaches an equilibrium state of low moisture content, the creep rate becomes substantially smaller than in a sealed specimen.

Refining the original BP model [1], we will extend the preceding formulation [2–4] from Parts 2 and 3 to creep of sealed and unsealed specimens at various temperatures that are kept constant during creep. A constitutive model for time-varying temperature (cf. [5]) can be obtained by generalizing the present formulation.

2. PROPOSED BASIC CREEP FORMULAE

To take temperature into account, Equations 2 to 8 of Part 2 [3] are generalized as follows:

$$J(t, t', \sigma) = q_1 + F(\sigma)C_0(t, t') \tag{1}$$

$$C_0(t, t') = q_2 Q'(t, t') + q_3 \ln[1 + (t_T - t'_e)] + q_4 \ln\left(\frac{t_T}{t'_e}\right) \tag{2}$$

in which the equivalent age at loading and the equivalent creep duration are calculated as

$$t'_e = \int_0^{t'} \beta_T(t'')\,dt'' \qquad t_T - t'_e = \int_{t'}^{t} \beta'_T(t'')\,dt'' \tag{3}$$

Based on activation energy theory,

$$\beta_T = \exp\left[\frac{U_h}{R}\left(\frac{1}{T_0} - \frac{1}{T}\right)\right] \tag{4}$$

$$\beta'_T = \exp\left[\frac{U_c(t - t')}{R}\left(\frac{1}{T_0} - \frac{1}{T}\right)\right] \tag{5}$$

with

$$U_c(t - t') = U_0 + U_1 \ln[1 + (t - t')] \tag{6}$$

The function from Equation 5 of Part 2 [3] describing the ageing viscoelastic compliance is generalized as

$$Q'(t, t') = Q_f(t'_e)\left[1 + \left(\frac{Q_f(t'_e)}{Z(t_T, t'_e)}\right)^{r(t'_e)}\right]^{-1/r(t'_e)} \tag{7}$$

Here T = temperature and T_0 = reference temperature (absolute temperatures, in K), U_h = activation energy of cement hydration, U_c = activation energy of creep describing the acceleration of creep rate due to temperature increase, and R = gas constant. The typical value of U_h/R is 4000 K, which is indicated by the test data of Maréchal [6]. The equivalent hydration period (or maturity) at the moment of load application, t'_e, represents the period needed at reference temperature T_0 to achieve the same degree of cement hydration as that achieved at actual temperature T during the actual time

0025–5432/92 © RILEM

period t' up to the moment of loading. The equivalent (effective) creep duration t_T represents the creep duration at reference temperature T_0 that gives the same creep strain as that obtained after load duration $t - t'$ at actual temperature T.

Equations 3–5 reflect the fact that the temperature effect on basic creep is twofold [7,8]: (a) an increase in temperature increases the creep rate, but (b) it also accelerates hydration, i.e. ageing. These effects, modelled by two different activation energies, characterizing different thermally activated processes, oppose each other. When young concrete is heated (below 100°C) well before it is loaded, the equivalent hydration period t'_e for the moment of load application may be sharply increased, which tends to offset the subsequent increase of creep rate due to heating. On the other hand, when old concrete is heated, the change in t'_e has little effect on the subsequent creep, and so a strong increase of creep with temperature takes place. Modelling of both these opposing effects is essential for successful representation of test data.

Both types of temperature effect are described in terms of activation energies, while in the original BP model [1] only the effect of temperature on t'_e was described in terms of activation energy. This is made possible by recognizing that the activation energy of creep, U_c, is not constant but increases with loading duration, as detected by Bažant and Wu [8]. This may be explained by hypothesizing that the bonds whose rupture and reformation cause long-time creep have a higher activation energy (i.e. are stronger) than those causing short-time creep.

The present model is intended for the temperature range from −20 to 140°C.

3. PREDICTION OF MATERIAL PARAMETERS FROM CONCRETE COMPOSITION AND STRENGTH

By analysis of experimental data, the following formulae were obtained:

$$\frac{U_0}{R} = \frac{130(f'_c)^{0.7}}{c^{0.8}(w/c)^{0.7}} \qquad \frac{U_1}{R} = 0.2\frac{U_0}{R} \tag{8}$$

in which c = cement content in lb ft^{-3} (lb ft^{-3} = 16.02 kg m^{-3}), w/c = water/cement ratio, f'_c = 28-day standard cylinder strength in psi (psi = 6895 Pa), and U_0/R, U_1/R are obtained in kelvins.

Equation 8 reflects the fact that an increase in strength makes the temperature effect milder, i.e. the activation energy of creep higher. An increase in cement content and in water/cement ratio makes creep more sensitive to temperature, i.e. lowers the activation energy.

4. COMPARISONS WITH BASIC CREEP TEST DATA

Figs 1–4 show the comparisons of the present formulae with various important test data from the literature [9–21]. Overall, the fit of the test results is better than with previous models. Again, the errors seen are caused mainly by the prediction of material parameter values from the mix composition and strength of concrete.

For some data sets, certain important information was not reported and, therefore, had to be assumed. For instance, for the data of England and Ross [13] it was assumed that heating was applied at the age of 10 days, simultaneously with load application (i.e. without any heat stabilization period before the test). Also, the initial 'elastic' strains at elevated temperatures were assumed to be proportional to the values measured by Maréchal [6]. When unspecified, the unit weight of concrete and the applied stress have been assumed as 150 lb ft^{-3} (2403 kg m^{-3}) and 30% of 28-day cylinder strength, respectively. For the tests of Da Silveira and Florentino [11], it was assumed that the heat was applied three days before loading. For Zielinski and Sadowski's data [21], the initial elastic strains, which had not been reported, were assumed to be 2.2×10^{-7} psi^{-1} (3.19×10^{-5} MPa^{-1}). For Nasser and Neville's data [18,19], the sand/gravel ratio was not available, and was assumed as 2/3; also, the initial elastic strains were assumed with the value 2.4×10^{-7} psi^{-1} (3.48×10^{-5} MPa^{-1}). Nasser and Neville [18,19] mentioned that E was not a function of temperature; therefore, the value of initial elastic strains has been found by optimized fits of creep data for normal temperature (21°C). The E value was reported to increase by 22% from t' = 14 days to t' = 365 days, and so the value of $J(t' + 0.001, t')$ was assumed to increase in proportion. Moreover, these data indicated a 22% increase of the elastic modulus upon heating, independently of the curing temperature. However, this conflicts with other work [6,22]. The deviations from test data in Figs 1–4 must be judged in the light of the preceding remarks.

Table 1 lists the coefficients of variation of the deviations of the hand-smoothed data curves from the present formulae, as well as the overall coefficient of

Table 1 Coefficients of variation for deviations of formulae from hand-smoothed data on temperature effect on basic creep

Test data	$\bar{\omega}$
Arthanari and Yu [10]	12.2
Browne [9]	22.2
Da Silveira and Florentino [11]	24.4
England and Ross [13]	12.2
Hannant [12]	9.6
Johansen and Best [14]	12.4
Kommendant *et al.* [17]	11.0
McDonald [16]	24.1
Nasser and Neville [18]	11.0
Nasser and Neville [19]	15.1
Seki and Kawasumi [15]	14.5
York *et al.* [20]	20.2
Zielinski and Sadowski [21]	8.0
$\bar{\omega}_{all}$ = 17.5	

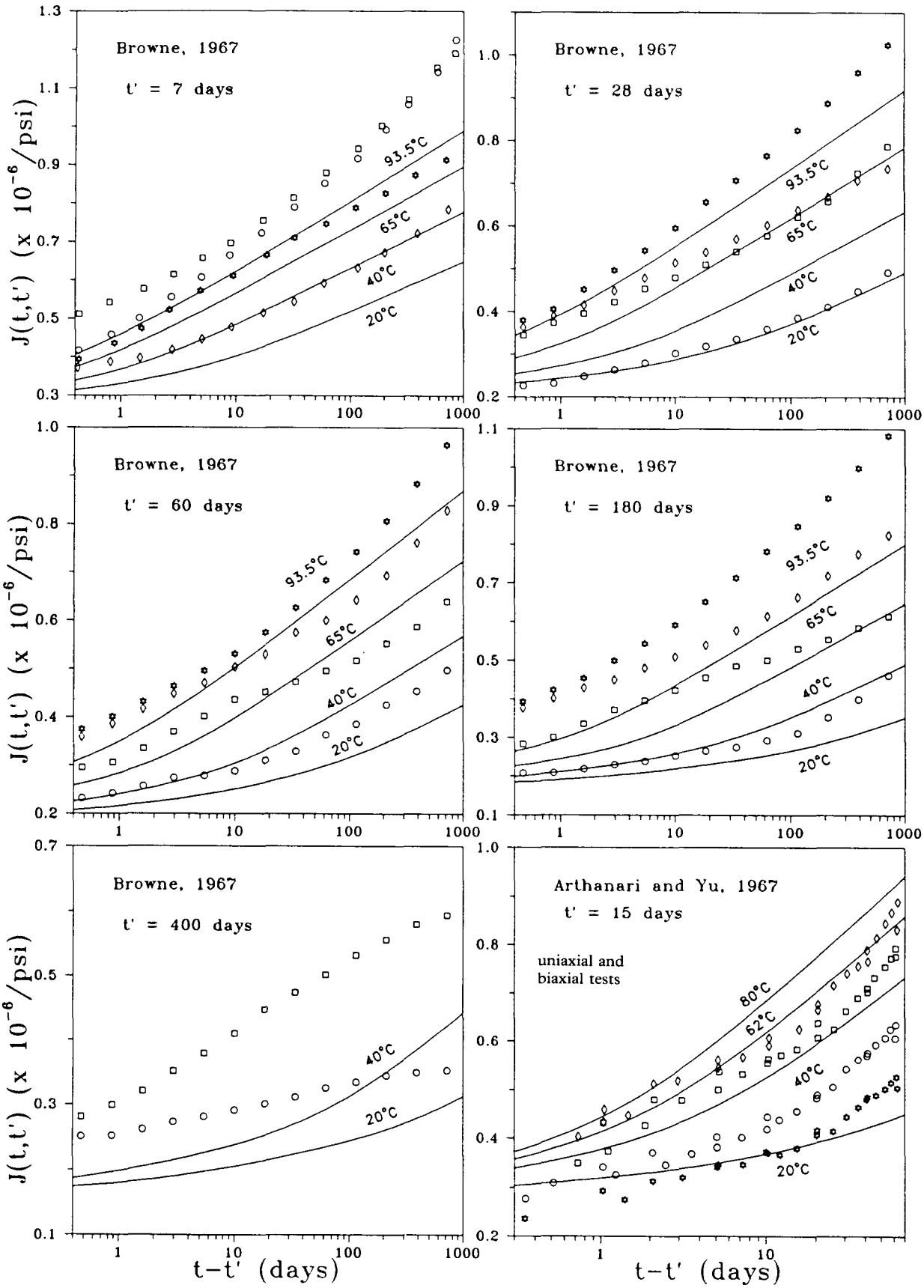

Fig. 1 Predictions of temperature effect on basic creep and data by Arthanari and Yu [10] and Browne [9].

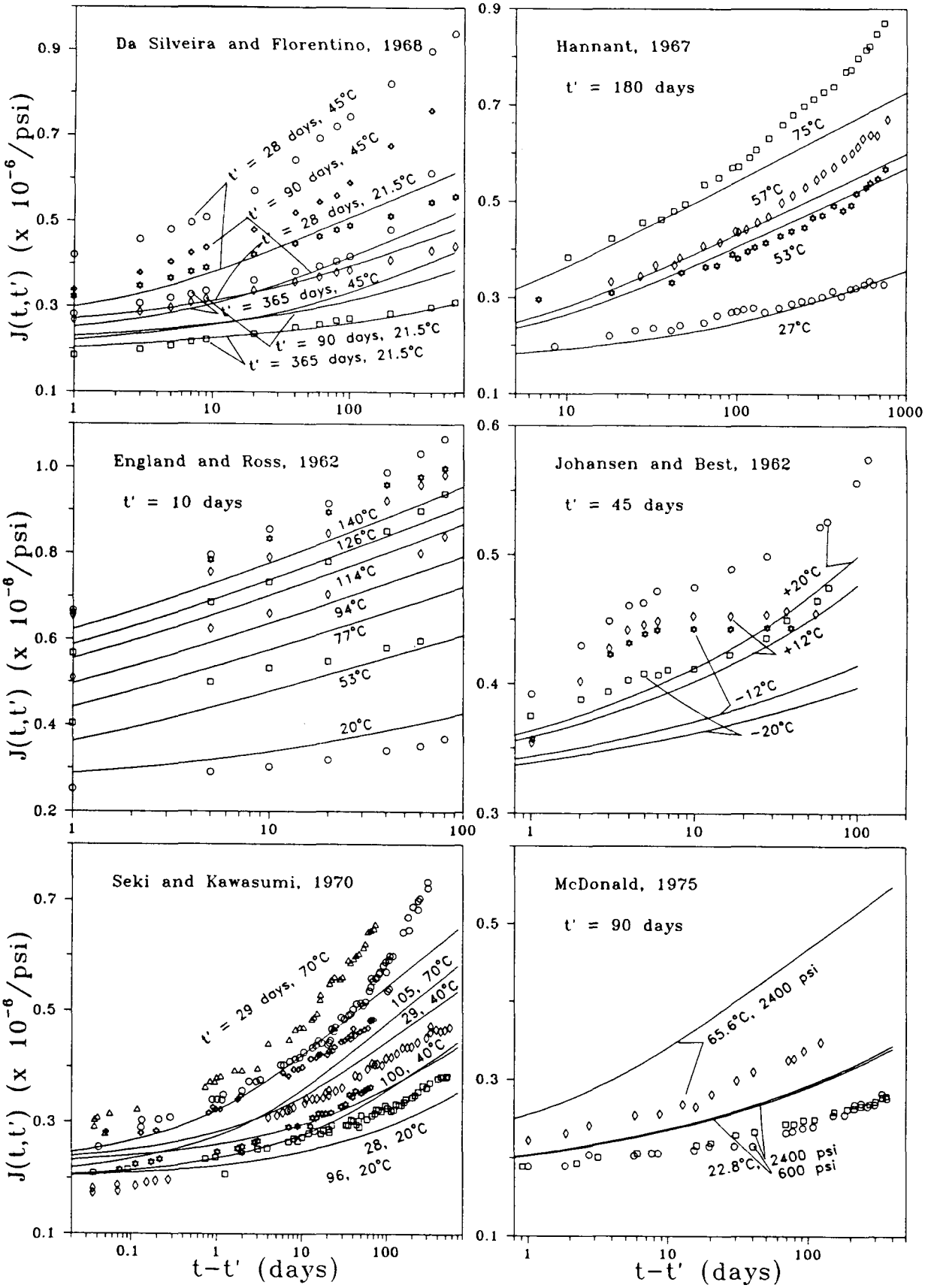

Fig. 2 Predictions of temperature effect on basic creep and data by Da Silveira and Florentino [11], England and Ross [13], Hannant [12], Johansen and Best [14], McDonald [16] and Seki and Kawasumi [15].

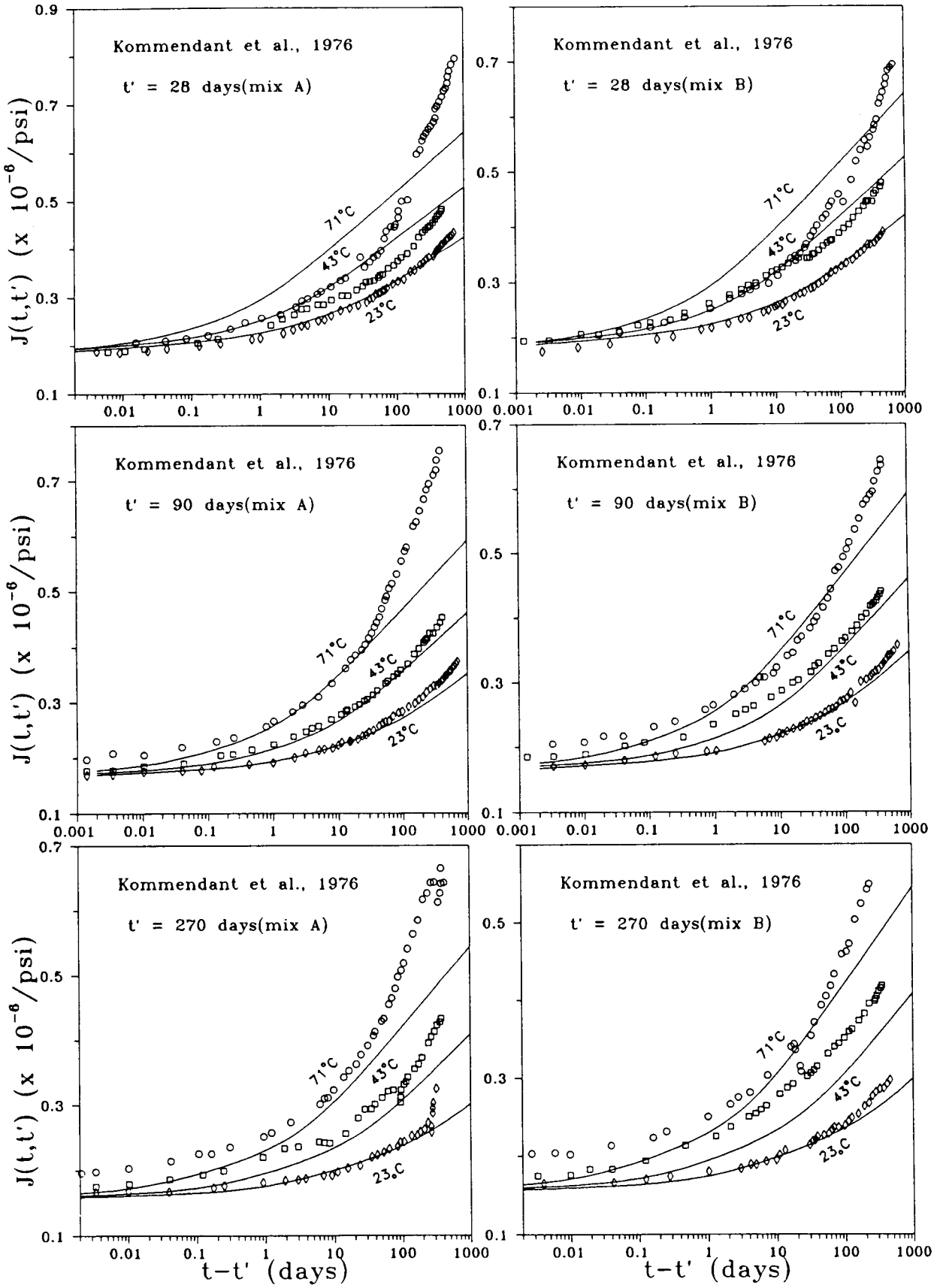

Fig. 3 Predictions of temperature effect on basic creep and data by Kommendant *et al.* [17].

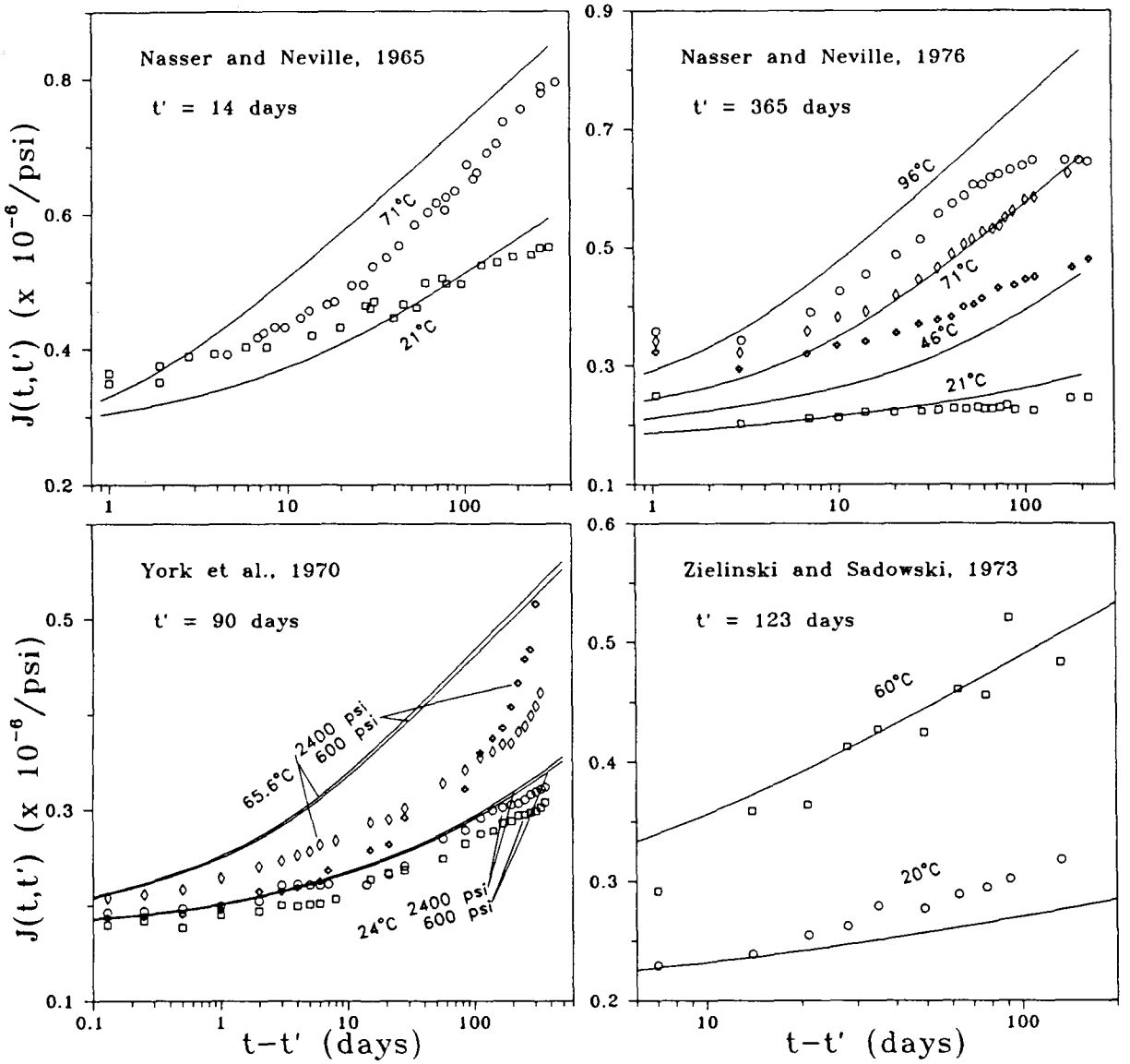

Fig. 4 Predictions of temperature effect on basic creep and data by Nasser and Neville [18,19], York *et al.* [20] and Zielinski and Sadowski [21].

variation. These values were calculated in the same manner as in Parts 1–3 [2–4], described in detail in Part VI of Bažant and Panula [1].

5. IMPROVEMENT OF BASIC CREEP PREDICTION FROM SHORT-TIME MEASUREMENTS

As emphasized before, for basic creep a great improvement of prediction is possible when even limited short-time measurements of creep at more than one temperature are made. In that case one first predicts all the material parameters as indicated so far, and then one replaces U_0 and U_1 by $k_a U_0$ and $k_a U_1$. Parameter k_a is then varied to find, by trial and error, the best fit of the given creep curves for different temperatures.

Likewise, when short-time measurements are available for curing at two significantly different temperatures, one first predicts all the parameters as indicated here and then replaces U_h by $k_h U_h$, and finds the value of k_h by trial and error so as to optimize the data fits.

6. PROPOSED DRYING CREEP FORMULAE

Since there is nothing special about room temperature, the formulae for creep at elevated temperatures should have the same form as those formulated for room temperature; only their coefficients should have different values. Therefore, the overall form of the compliance function in Equation 1 of Part 3 [4] is retained, while the components $C_d(t, t', t_0)$ and $C_p(t, t', t_0)$ are modified as follows:

Creep during drying

$$C_d(t, t', t_0) = q_5 k'_h \varepsilon_{sh\infty} \left[S\left(\frac{t_e - t_{e0}}{\tau_m}\right) - S\left(\frac{t''_e - t_{e0}}{\tau_m}\right) \right]^{1/2} \quad (9)$$

$$\tau_m = 2\left(1 + \frac{3.5}{(t_{e0})^{1/2}}\right)\left(1 + \frac{5}{(t'_e + t_{e0})^{1/2}}\right)^{-1} \tau_{sh} \quad (10)$$

Creep after drying

$$C_p(t, t', t_0) = 0.7k_h''\left[\left(\frac{1}{G(7 + t_{e0})} - 0.9^{1/2}\right)S\left(\frac{t_e'' - t_{e0}}{0.5\tau_m}\right) - S\left(\frac{t_e'' - t_{e0}}{5\tau_m}\right)\right]C_0(t, t') \quad (11)$$

Temperature dependence

$$t_e' = \int_0^{t'} \beta_T(t'')\,dt'' \quad (12)$$

$$t_e'' - t_0 = \int_{t_0}^{t'} k_T'(t'')\,dt'' \quad (13)$$

$$t_{e0} = \int_0^{t_0} \beta_T(t'')\,dt'' \quad (14)$$

$$t_e - t_{e0} = \int_{t_0}^{t} k_T'(t'')\,dt'' \quad (15)$$

Humidity dependence

$$k_h' = \int_0^{t} h^3(t'')\,dt'' \quad (16)$$

$$k_h'' = \int_0^{t} h^2(t'')\,dt'' \quad (17)$$

Here S is the shrinkage function defined in Equation 2 of Part 1 [2], h is the relative humidity and $C_0(t, t')$, $C_d(t, t', t_0)$ and $C_p(t, t', t_0)$ are the same as for basic creep and drying creep. However, the hydration period, drying duration and loading duration are accelerated according to the activation energy concept; β_T and k_T' are functions of temperature, the same as in Equation 10 of Part 1 [2] and Equation 3 above; t_e' represents the equivalent hydration period at the age at loading; t_e'' represents the equivalent period when the specimen is exposed to elevated temperature T; t_{e0} represents the equivalent hydration period when drying begins; t_e represents the effective age of concrete ($t_e - t_{e0}$ = equivalent loading duration), and k_h' and k_h'' are the same as in Equation 5 of Part 3 [4].

7. COMPARISONS WITH DRYING CREEP TEST DATA

The existing data on drying creep of heated concrete are quite limited. They deal mostly with concretes typical of reactor vessels. Comparisons with five test data sets from the literature [6,10,15,22,23] are presented in Fig. 5.

The most comprehensive and consistent data are those of Hickey [23]. The data of Seki and Kawasumi's tests [15] involved an unusual curing history, in which specimens were demoulded and exposed to (average) 50% relative humidity already at demoulding at 24 h of age (therefore, the strength of air-dried specimen was used in prediction). Also, the relative humidity was not controlled in these tests (only the approximate mean humidity was reported). This may have also been the reason why the measured basic creep curves $J(t, t')$ for $t' = 29$ and 105 days were unusually close to each other. The concrete used in these tests included a mixture with pozzolith, whose effect is not covered by the present model. This is probably the reason for the underestimation of creep for these data, already mentioned in Part 2 [3]. Nevertheless, the observed trend of the temperature effect is not predicted badly.

In the tests of Gross [22], which were of relatively short duration, the curves for 40, 60 and 80°C are strangely close to each other, compared to other tests. Also, the initial deformation appears to be influenced more than creep. In the data of Arthanari and Yu [10], the relative humidities for 20, 58, 84 and 102°C were not reported; they were assumed to be 50, 25, 3 and 1%, respectively (which are the theoretical humidity values achieved by heating if the mass content of water in the air is kept constant). The estimates obtained nevertheless appear to be adequate for high temperatures (84 and 102°C), probably because the humidities obtained by heating room air at constant moisture content are always close to zero at such temperatures. The initial elastic deformation was also not reported for these tests and had to be estimated. For this purpose, the creep values for very short times were compared with the corresponding creep values reported for sealed specimens of the same composition. The fact that the measured curves for 58 and 84°C cross each other must be due to random scatter and thus cannot be represented by formulas for the mean trend.

The tests of Maréchal [6] are special due to their relatively long preheating period (15 days) and a rather small specimen size. Since the drying time is proportional to the square of size, the small specimen size must have caused the specimens at high temperature to lose much of their water before load application, while at lower temperatures the 15-day period might not have sufficed to cause a large moisture loss, because of lower diffusivity. This might explain why the creep at 70°C was less than the creep at 50°C, although the source of the discrepancy might be partly random. The measured peak value of creep in these data occurred at roughly 50°C, while the present formulae give a peak at 70°C. This discrepancy could not be reduced without causing the temperature effect on creep to be too small for other data. It is mainly for these reasons that the fits of Maréchal's data are not very close, although the prediction of their basic trends is qualitatively correct. The use of a long preheating period in these data was useful for determining the value of U_h/R (Equation 4). The initial elastic deformation for Maréchal's tests was not reported as part of the creep test results [6]; however, the value given in Maréchal [24] was used since it probably referred to the same tests. The relative humidities and mix proportions were not reported and had to be assumed for these data.

The values of the coefficients of variation of the deviations of the predictions from the hand-smoothed measured creep curves are listed in Table 2, along with overall coefficient of variation for all the data.

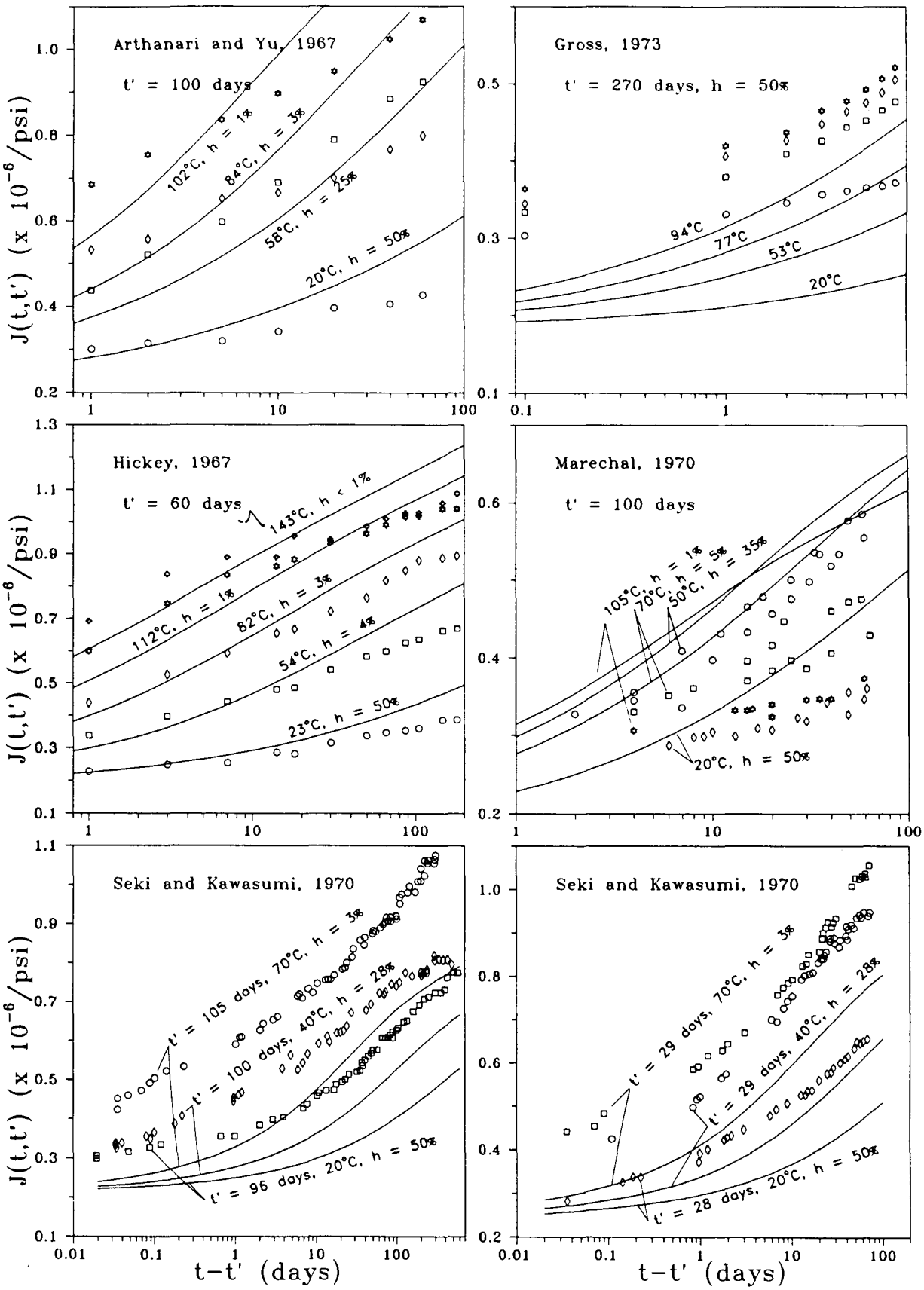

Fig. 5 Predictions of temperature effect on drying creep compared with test data by Arthanari and Yu [10], Gross [22], Hickey [23], Maréchal [6] and Seki and Kawasumi [15].

Table 2 Coefficients of variation for deviations of formulae from hand-smoothed data

Test data	$\bar{\omega}$
Arthanari and Yu [10]	17.3
Gross [22]	31.2
Hickey [23]	12.1
Maréchal [6]	31.8
Seki and Kawasumi [15]	34.1
$\bar{\omega}_{all} = 26.8$	

APPENDIX I: Basic information on tests of temperature effect on basic creep

Arthanari and Yu [10]. Slabs 12 in. × 12 in. (305 cm × 305 cm × 102 cm), cured under wet hessian for 7 days. The specimens, simulating mass-concrete, were sealed by epoxy resin and two coats of plastic emulsion paint. Loaded at the age of 15 days. Heating began 1 day before loading. 28-day cube strength = 6000 psi (41.4 N mm^{-2}). Ordinary Portland cement, Thames river gravel of size 3/16–3/8 inch (4.76–9.5 mm), water:cement:sand:coarse aggregate ratio = 0.564:1:1.125:2.625. Axial compressive stress = 1000 psi (6.9 N mm^{-2}).

Browne [9]. Cylinders 6 in. × 12 in. (152 cm × 305 cm) sealed at casting in 1/16 in. (1.6 mm) polypropylene jackets, cured at room temperature. Heating began 1 day before loading. Average 28-day cube strength = 7250 psi (50 N mm^{-2}). Ordinary Portland cement, content 418 kg m^{-3}; water:cement:sand:coarse aggregate ratio = 0.42:1:1.45:2.95. Axial compressive stress = 2116 psi (14.6 N mm^{-2}).

Da Silveira and Florentino [11]. Prisms 20 cm × 20 cm × 60 cm in copper jackets. Heat is assumed to have begun 3 days before loading. 8-day cube strength = 297 kg cm^{-2} (29.1 N mm^{-2}); modified Portland cement (similar to ASTM type II), content 314.6 kg m^{-3}; water:cement:sand:coarse aggregate ratio = 0.5:1:2.35:3.84.

England and Ross [13]. Cylinders 4.5 in. × 12 in. (114 cm × 305 cm), demoulded at 1 day, placed under water for additional 3 days, then stored at 17°C and 90% relative humidity until tested at age of 10 days in sealed state. The seal was a polyester resin, with fibreglass reinforcement. 14-day 4-in. (102 mm) cube strength = 5500 psi (37.5 N mm^{-2}); water:cement:sand:coarse aggregate ratio = 0.45:1:2:4.

Hannant [12]. Cylinders 4$\frac{1}{8}$ in. × 12 in. (105 cm × 305 cm) cured for 24 h in moulds under wet rugs, then 5 months under water at 20°C, and then for one month sealed in copper. Heating rates about 10°C h^{-1}. Heated for 24 h before loading. 28-day cube strength = 9350 psi (64.5 N mm^{-2}). Sulphate-resisting Portland cement, max. size of aggregate 3/4 in. (19 mm); water:cement:sand:coarse aggregate ratio = 0.47:1:1.845:2.655. Axial compressive stress = 2000 psi (13.8 N mm^{-2}).

Johansen and Best [14]. Cylinders 10 cm × 30 cm and 15 cm × 30 cm, cast in steel moulds and demoulded at age of 1 day, then stored at 100% relative humidity and 20°C. At age of 42 days, specimens were sealed and moved to test environment. After 3 days of stabilization, specimens were loaded at 30% of ultimate strength. 42-day strength = 185 kg cm^{-2} (2633 psi); normal Portland cement, max. size of aggregate 3/8 in. (9.5 mm); water:cement:sand:coarse aggregate ratio = 0.7:1:3.5:3.5. Axial compressive stress = 790 psi (5.5 N mm^{-2}).

Kommendant et al. [17]. Cylinders 6 in. × 16 in. (152 mm × 305 mm) sealed with butyl rubber and cured at 73°F (23°C), until 5 days before the age of loading. The specimens were then heated to test temperatures 100 and 160°F (43 and 71°C) at the rate of 24°F per day (13.3°C per day). 28-day cylinder strengths = 6590 psi (45.4 N mm^{-2}) and 6700 psi (46.2 N mm^{-2}); water:cement:sand:coarse aggregate ratios = 0.38:1:1.73:2.61 and 0.38:1:1.65:2.38, respectively; cement Medusa ASTM type II, content 419 kg cm^{-3}; max. size of aggregate 1.5 in. (38.1 mm). Axial compressive stress = 32% of 28-day strength.

McDonald [16]. Cylinders 6 in. × 16 in. (152 mm × 406 mm), demoulded after 24 h and placed in fog room. After 24 h another coat of epoxy, and sealed in copper. After age of 83 days, specimens recoated with epoxy, sealed in neoprene, and placed to test temperature. Loaded at the age of 90 days. 28-day cylinder strength = 6300 psi (43.4 N mm^{-2}); cement type II, content 404 kg m^{-3}; limestone, max. size of aggregate 0.75 in. (19 mm); water:cement:sand:coarse aggregate ratio = 0.425:1:2.03:2.62. Axial compressive stresses = 600 and 2400 psi (4.1 and 16.6 N mm^{-2}).

Nasser and Neville [18]. Cylinders 3 in. × 9.25 in. (76 cm × 235 cm), sealed in polypropylene jackets, stored from the age of 24 h onwards in water bath at desired temperature and loaded at 14 days. 14-day cylinder strength = 5660 psi (39.0 N mm^{-2}) measured on test specimens; cement type III, content 320 kg m^{-3}; max. size of aggregate 3/4 in. (19 mm); water:cement:aggregate ratio = 0.6:1:7.15. Axial compressive stress 1950 psi (13.4 N mm^{-2}).

Nasser and Neville [19]. Cylinders 3 in. × 9.25 in. (76 cm × 235 cm) stored in water bath at 70°F (21°C) up to 1 week before load application. All specimens were under water while loaded. 1-year cylinder strength = 7250 psi (50 N mm^{-2}) on test specimens; cement type III, content 320 kg m^{-3}; max. size of aggregate 3/4 in. (19 mm); water:cement:aggregate ratio = 0.6:1:7.15; stress/strength ratio 45%.

Seki and Kawasumi [15]. Cylinders 150 cm × 600 cm (6 in. × 24 in.) were cast into copper jackets. Specimens cured at 20°C. Temperature 40°C applied at the ages of 28 days and 97 days and loaded at 29 days and 100 days. Temperature 70°C applied at the ages of 27 days and 104 days, and loaded at 29 days and 105 days, respectively. 28-day cylinder strength = 445 kg cm^{-2} in water, 321 kg cm^{-2} for sealed specimens, and 279 kg cm^{-2} for unsealed specimens; normal Portland cement content 343 kg m^{-3}. Pozzolith was added to the mixture (0.25% of cement content). Max. size of aggregate 40 mm;

water:cement:sand:coarse aggregate ratio = 0.4:1:1.761:3.834. Axial compressive stress 1280 psi (8.8 N mm^{-2}).

York et al. [20]. Cylinders 6 in. × 16 in. (152 mm × 406 mm), sealed 48 h after casting and then cured for 81 days at 75°F (24°C). At the age of 83 days specimens sealed in neoprene jackets, and exposed to test temperature. Loaded at 90 days. 28-day cylinder strength = 6460 psi (44.6 N mm^{-2}); Portland cement type II, content 404 kg m^{-3}; max. size of aggregate 0.75 in. (19 mm); water:cement:sand:coarse aggregate ratio = 0.425:1:2.03:2.62. Axial compressive stress 2400 psi (16.6 N mm^{-2}).

Zielinski and Sadowski [21]. Cylinders 160 mm × 480 mm, within first 70 days stored at 100% relative humidity and 20–23°C, then sealed with rubber coat. After 120 days, specimens heated and loaded 3 days later. 120-day cylinder (16 cm × 16 cm) strength = 430 kg cm^{-2}; ordinary Portland cement type I, content 450 kg m^{-3}; max. size of aggregate 20 mm; water:cement:aggregate ratio = 0.425:1:4.154. Axial compressive stress up to 150 kgf cm^{-2}.

APPENDIX II: Basic information on tests of temperature effect on drying creep

Arthanari and Yu [10]. Slabs 12 in. × 12 in. × 4 in. (305 cm × 305 cm × 102 cm), cured under water until 3 days before loading. Loaded at the age of 100 days. Heating began 1 day before loading. The reported biaxial test data were transformed to equivalent uniaxial ones, assuming Poisson's ratio to be 0.2, both for elasticity and creep. The initial (elastic) values of $J(t, t')$ at $t - t' = 0.001$ day and 20, 58, 84 and 102°C were assumed to be 2.5, 2.73, 2.88, 2.98 × 10^{-7} psi^{-1} (3.6, 3.96, 4.18, 4.32 × 10^{-5} MPa^{-1}); the corresponding relative humidities were assumed as 70, 50, 2, 1%; 28-day cube cold strength = 6000 psi (41.4 N mm^{-2}); ordinary Portland cement, its content assumed as 437 kg cm^{-3}, Thames river gravel of size 3/16–3/8 in. (4.73–9.45 mm), max. size of aggregate 3/8 in. (9.5 mm); water:cement:sand:coarse aggregate ratio = 0.564:1:1.125:2.625. Axial compressive stress = 1000 psi (6.9 N mm^{-2}).

Hickey [23]. Cylinders 6 in. × 16 in. (152 mm × 152 mm), in moulds for 24 h at 73°F (23°C); then stripped and cured in a fog room at 73°F (23°C) for 1 month; then exposed to 50% relative humidity at 73°F (23°C) for another month. One day before starting the elevated temperature tests the specimens were wrapped with fibreglass insulation (to minimize temperature changes). The specimens were loaded at the age of 2 months. Immediately after loading, the chamber temperature was slowly increased to the test temperature over a period of about 24 h. 39-day strength of specimens = 7700 psi (51.7 N mm^{-2}); cement type V, content 332 kg m^{-3}, with pozzolan (83 kg m^{-3}), max. size of aggregate 1 in. (25 mm); water:cement:sand:coarse aggregate ratio = 0.468:1:1.775:3.864. The applied stress assumed as 30% of 28-day cylinder strength.

Gross [22]. Cylinders 60 mm × 180 mm were stored in water up to 7 days, then kept under damp hessian for 4 weeks, thereafter in the air at 50% relative humidity and 20°C. Specimens were preheated for one day at the relevant temperature. Load applied at the age of 9 months. 28-day average cube strength = 42 N mm^{-2}; ordinary Portland cement, its content assumed as 387 kg cm^{-3}. Aggregate: Thames river deposits, max. size of aggregate 9.5 mm; water:cement:sand:coarse aggregate ratio = 0.4:1:1.761:3.834. Axial compressive stress = 8.4 N mm^{-2}.

Maréchal [6]. Prisms 70 mm × 70 mm × 280 mm, cured in water for 1 year, then heated at 0.25°C h^{-1} to the test temperature. Temperature stabilization period: 15 days before loading. Specimens at temperatures 20, 50, 70, 105, 150°C were assumed to dry at 50, 35, 3 and 1% relative humidity. Cement content 400 kg m^{-3}. The following was assumed: water:cement:sand:gravel ratio 0.5:1:2:2, 28-day average cylinder strength 5500 psi (37.9 N mm^{-2}), applied stress 30% of 28-day cylinder strength. The initial (elastic) values of $J(t, t')$ at elevated temperatures were evaluated using Maréchal's data [6].

Seki and Kawasumi [15]. Cylinders 150 mm × 600 mm (6 in. × 24 in.) were demoulded after 24 h and cured at 20°C and 50% relative humidity, sealed at the top and bottom. The temperature 40°C was applied at the age of 28 days and 97 days and loaded at 29 days and 100 days, respectively. Relative humidity was not controlled; its average was about 28%. Temperature 70°C was applied at the age of 27 days and 104 days; samples were loaded at 29 and 105 days. Relative humidity was not controlled, but was about 3%. 28-day cylinder strengths = 445 kg cm^{-2} in water, 321 kg cm^{-2} for sealed specimen and 279 kg cm^{-3} for unsealed specimen; ordinary Portland cement, content 343 kg m^{-3}. Fine aggregate natural sand from the Fuji-Gawa river, coarse aggregate from the Ara-Kawa river, max. size 40 mm; water:cement:sand:coarse aggregate ratio = 0.4:1:1.761:3.834. Pozzolith was added to the mixture (0.25% of cement content). Axial compressive stress 1280 psi (8.8 N mm^{-2}).

REFERENCES

1. Bažant, Z. P. and Panula, L., 'Practical prediction of time-dependent deformations of concrete'. Part I and II: *Mater. Struct.* **11**(65) (1978) 307–328. Parts III and IV: *ibid.* **11**(66) (1978) 415–434. Parts V and VI: *ibid.* **12**(69) (1979) 169–183.
2. Bažant, Z. P., Kim, J.-K. and Panula, L., 'Improved prediction model for time-dependent deformations of concrete: Part 1 – Shrinkage', *ibid.* **24** (1991) 327–345.
3. Bažant, Z. P. and Kim, J.-K., 'Improved prediction model for time-dependent deformations of concrete: Part 2 – Basic creep', *ibid.* **24** (1991) 409–421.
4. *Idem*, 'Improved prediction model for time-dependent deformations of concrete: Part 3 – Creep at drying', *ibid.* **25** (1992) 21–28.
5. Bažant, Z. P., 'Material modes for structural creep analysis', in 'Mathematical Modeling of Creep and Shrinkage of Concrete', edited by Z. P. Bažant (Wiley, Chichester, 1988) pp. 99–215.
6. Maréchal, J. C., 'Fluage du béton en fonction de la

température', *Ann. Inst. Techn. Bâtiment Trav. Pub.* **23**(266) (1970) 13–24.
7. Bažant, Z. P., 'Theory of creep and shrinkage in concrete structures: a precis of recent developments', *Mechanics Today* **2** (1975) 1–93.
8. Bažant, Z. P. and Wu, S. T., 'Thermoviscoelasticity of aging concrete', *J. Engnr. Mech. ASCE* **100**(EM3) (June 1972) 575–597.
9. Browne, R. D., 'Properties of concrete in reactor vessels', in Proceedings of Conference on Prestressed Concrete Pressure Vessels, group C (Institution of Civil Engineers, London, 1967) pp. 11–31.
10. Arthanari, S. and Yu, C. W., 'Creep of concrete under uniaxial and biaxial stresses at elevated temperatures', *Mag. Concr. Res.* **19**(60) (1967) 149–155.
11. Da Silveira, A. and Florentino, C., 'Influence of temperature on creep of mass concrete', in 'Temperature and Concrete', ACI Special Publication SP-25 (American Concrete Institute, Detroit, 1971) pp. 173–189.
12. Hannant, D. J., 'Strain behaviour of concrete up to 95°C under compressive stresses', in Proceedings of Conference on Prestressed Concrete Pressure Vessels, group C (Institution of Civil Engineers, London, 1967) pp. 57–71.
13. England, G. and Ross, A. D., 'Reinforced concrete under thermal gradients', *Mag. Concr. Res.* **14**(4) (1962) 5–12.
14. Johansen, R. and Best, H., 'Creep of concrete with and without ice in the system', *Bull. RILEM* **16** (September 1962) 47–57.
15. Seki, S. and Kawasumi, M., 'Creep of concrete at elevated temperatures', in 'Concrete of Nuclear Reactors' Vol. I, ACI Special Publication SP-34 (American Concrete Institute, Detroit, 1972) pp. 591–638.
16. McDonald, J. E., 'Time-dependent deformation of concrete under multiaxial stress conditions', Technical Report C-75-4 (Concrete Laboratory, US Army Engineering Waterways Experiment Station, Vicksburg, Miss., 1975).
17. Kommendant, G. J., Polivka, M. and Pirtz, D., 'Study of concrete properties for prestressed concrete reactor vessels, final report – part II, Creep and strength characteristics of concrete at elevated temperatures', Report No. UCSESM 76-3 to General Atomic Company (Department of Civil Engineering, University of California, Berkeley, 1976).
18. Nasser, K. W. and Neville, A. M., 'Creep of concrete at elevated temperatures', *ACI J* **62** (December 1965) 1567–1579.
19. *Idem*, 'Creep of old concrete at normal and elevated temperatures', *ibid.* **64** (February 1967) 97–103.
20. York, G. P., Kennedy, T. W. and Perry, E. S., 'Experimental investigation of creep in concrete subjected to multiaxial compressive stresses and elevated temperatures', Research Report 2864-2 to Oak Ridge National Laboratory (Department of Civil Engineering, University of Texas, Austin, June 1970); see also 'Concrete for Nuclear Reactors', American Concrete Institute Special Publication No. 34 (1972) pp. 647–700.
21. Zielinski, J. L. and Sadowski, A., 'The influence of moisture content on the creep of concrete at elevated temperatures', in Proceedings of 2nd International Conference on Structural Mechanics in Reactor Technology, edited by T. A. Jaeger (Commission of European Communities, Berlin, 1973) pp. 1–8.
22. Gross, H., 'On high-temperature creep of concrete', *ibid.* Paper H6/5.
23. Hickey, K. B., 'Creep, strength, and elasticity of concrete at elevated temperatures', Report No. C-1257, Concrete and Structural Branch, Division of Research, United States Department of the Interior (Bureau of Reclamation, Denver, Colorado, 1967).
24. Maréchal, J. C., 'Variations in the modulus of elasticity and Poisson's ratio with temperature', in 'Concrete for nuclear reactors', Vol. I, ACI Special Publication SP-34 (American Concrete Institute, Detroit, 1972) pp. 495–503.

RESUME

Modèle amélioré de prédiction des déformations du béton en fonction du temps. 4ème partie – Effet de température

Dans ce volet, on présente un modèle BP perfectionné pour les effets de la température sur le fluage de base et le fluage au séchage du béton. L'effet de température sur le fluage de base se produit par l'intermédiaire de deux énergies d'activation différentes, une pour l'effet de l'accroissement de la température sur la vitesse de l'hydratation, qui cause une diminution du fluage, et l'autre pour l'effet de l'accroissement de la température sur la vitesse du fluage, qui cause un accroissement du fluage.

L'opposition de ces deux effets de la température constitue une caractéristique nécessaire pour une bonne concordance avec les données d'essai. L'erreur la plus importante dans le fluage de base reste due à la prédiction des paramètres du matériau à partir de la composition et de la résistance du béton, erreur qui peut être éliminée en effectuant des essais limités de fluage de base à court terme à des températures différentes.

Des comparaisons avec 13 séries d'essai différentes sélectionnées dans la littérature montrent une concordance satisfaisante, supérieure à celle obtenue avec les modèles précédents. Cependant, en même temps, le champ d'application de ce modèle est plus large. L'effet de la température sur le fluage des éprouvettes en cours de séchage est assez différent car le chauffage entraîne une perte d'humidité dans les éprouvettes à l'air libre.

On présente ici des formules de prédiction qui modifient celles utilisées pour le fluage en séchage à température ambiante sur la base du concept d'activation de l'énergie, et qui prennent en compte l'effet du chauffage sur la perte d'humidité. Des comparaisons avec les données d'essai limitées dont on dispose montrent une concordance satisfaisante. On n'a pas introduit d'autres paramètres du matériau en relation avec le comportement et la résistance du béton pour le fluage au séchage.